Proceedings of the ASME 2017 36th International Conference on Ocean, Offshore and Arctic Engineering
OMAE2017
June 25-30, 2017, Trondheim, Norway

OMAE2017-61802

INITIAL DESIGN OF A DOUBLE CURVED FLOATING BRIDGE AND GLOBAL HYDRODYNAMIC RESPONSES UNDER ENVIRONMENTAL CONDITIONS

Ling Wan*
Department of Civil and Environmental Engineering, Faculty of Engineering, National University of Singapore

Allan Ross Magee
Department of Civil and Environmental Engineering, Faculty of Engineering, National University of Singapore

Øyvind Hellan**
Sintef Ocean
Trondheim, Norway

Watn Arnstein**
Sintef Ocean
Trondheim, Norway

Kok Keng Ang
Department of Civil and Environmental Engineering, Faculty of Engineering, National University of Singapore

Chien Ming Wang
Department of Civil and Environmental Engineering, Faculty of Engineering, National University of Singapore

ABSTRACT

In this paper, a floating bridge concept is proposed. This bridge concept comprises a two oppositely curves in plan, which enables the cancellation of the axial forces at the bridge as one arch will be under compression while the other arch is in tension due to environmental forces acting in one direction. The road deck is carried by truss structures that are kept above the water by several elliptical cylindrical pontoons. To reduce drag load, the cross sectional area facing the current is reduced as much as possible, while the buoyancy is kept the same based on the initial weight estimation. Initial design consideration and methodology of a double curved floating bridge is presented, and a numerical model is established for analyzing this concept. Hydrodynamic and structural dynamic aspects are included in the numerical model. Parametric study of the bridge structural rigidity is performed to investigate the effect to the responses. White noise, regular and irregular wave simulations are carried out to investigate the dynamic responses of the floating bridge under different conditions.

INTRODUCTION

Floating bridges are more feasible than bottom fixed bridges in crossing cannel or fjord under conditions that the water depth is deep and the span is very long, or under conditions with very soft seabed. In addition, marine environment can be well protected by floating bridge compared with fixed bridge solution. The existing floating bridges are mainly categorized into the following configurations [1, 2]: floating bridges supported by single continuous pontoon such as Lacey V. Murrow Bridge and Hood Canal Bridge in USA, or the bridge is supported by several separated pontoons such as Bergsoysund bridge [3] and Nordhordland bridge built in Norway, and submerged floating tunnel proposed for crossing the Norwegian fjords [4]. The horizontal stiffness can be provided by mooring system or curved shape of the bridge itself [3]. The vertical stiffness can be achieved by pontoon hydrostatic stiffness, or the tension leg type of mooring system. Besides that, the suspension bridge or cable-stayed bridge configurations can also be applied in the floating bridge to provide additional support. For analysis of single continuous pontoon bridge, frequency or time domain method considering the hydroelasticity can be used [5]. For separated pontoons, a decoupled hydro-structural model can be built based on the Boundary Element Method and Finite Element Method where beam elements are used to model the bridge deck [6].

The floating bridge concept studied here is a double-curved floating bridge, supported by 6 small pontoons and 2 large pontoons as shown in Figure 1. No mooring system in water is used. The water depth of the deployment is around 20 m, which is quite a shallow water condition. The reason for developing floating bridge in this condition is due to the soft seabed and due to the consideration of marine environmental protection. The bridge ends are connected to the onshore parts, and the horizontal

* Previous affiliation: Norwegian University of Science and Technology (NTNU)
Email: ling.wan@ntnu.no

**Previous affiliation: Marintek, Norway

stiffness is achieved by the curved shape and the end connections. This paper focuses on the initial investigation of the bridge pontoons, bridge global structural parameters including bridge sectional rigidity in axial, bending and torsion, and further the global dynamic responses under different environmental conditions. The global coordinate system as shown in Figure 1 is used, with z direction is perpendicular to the still water surface, and is pointing upward, x direction pointing to the transverse direction of the bridge, while y direction follows the right-hand rule, and is pointing to the bridge longitudinal direction. For the analysis of the local bridge deck beam, local coordinate system is used. The local coordinate system of the bridge deck beam element has the same z direction as the global coordinate system, but the y direction follow the exact bridge road directions with the same y positive direction. For concise descriptions, different pontoons are named by their corresponding positions as shown in Figure 1. As the bridge has symmetry along both X and Y axis, if the pontoon number is not indicated in this paper, it means the CTRL PT1, YPOS PT1 and YPOSSIDE PT are referred to. Truss structure is initially designed as the supporting structure for the bridge deck and is connected to the pontoons in the bottom. The two curved truss form a closed circle close to the two ends of the floating bridge to achieve cancellation effect of the tensions in the y direction as shown in Figure 2.

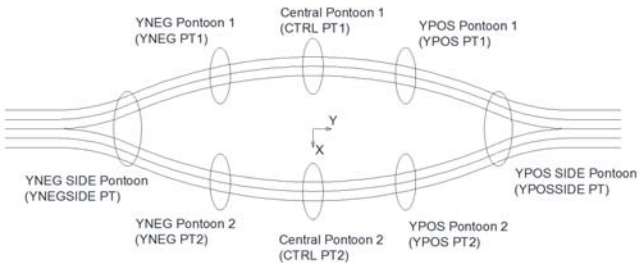

Figure 1 Plan view of the floating bridge concept proposed in this paper

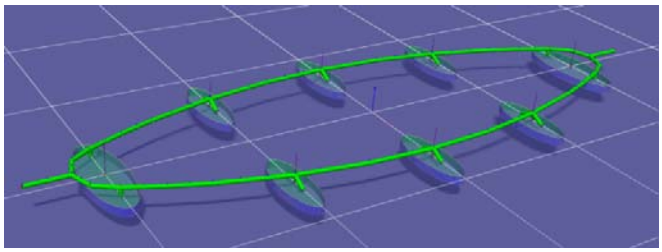

Figure 2 Numerical model of the two curved floating bridge

In this paper, the pontoon design in terms of stability, construction and installation is firstly considered; then, bridge structural parametric study is performed in terms of static analysis, eigenvalue analysis and dynamic analysis; at last, global dynamic response prediction of the floating bridge under different environmental conditions is performed, and the design criteria is used to verify the design. The numerical modelling is performed in SIMA, which contains SIMO/RIFLEX, which can used to solve coupled slender structural and hydrodynamic problems.

PONTOON DESIGN

Semi-submerged type of pontoons are used in this study. The important design basis for the pontoon is the dynamic properties of the bridge, including the bridge beam sectional rigidity, mass distribution, deflection requirement etc. However, in the initial design of this concept, all these information does not exists, so some basic parametric study is necessary to achieve proper design. In addition, some other considerations including current force reduction on the pontoons, stability during transportation and installation may be marginal important, and can be considered at the same time.

Elliptical cylinder shape with cross sectional area that facing current direction as small as possible is deployed for the reduction of the current drag loads, as frequent current cases will be encountered in the location of deployment. From initial study and estimation of the floating bridge weight, the pontoon material will be assumed to be light weight concrete. The pontoons are designed to have 3m freeboard and 6m draft trying to avoid severe water on deck or water exit of the pontoons. The stability of the pontoon is an important design parameter from installation point of view. From this aspect, the water plane area of the pontoon should be designed so that it can provide enough metacentric height during transportation and installation phases. In addition, the C.O.G of the pontoon itself should be as low as possible to accommodate higher C.O.G of the bridge deck so that the total C.O.G does not exceed the metacenter. For the consideration of various constraints by weight and buoyancy balance, stability requirements, cross sectional area requirement facing the current, some iteration calculations are performed. The pontoons parameters are selected as shown in Table 1. It is noted that these estimations are just based on the stability and current force considerations, overall hydrodynamic and structural optimization is not taken into consideration. Further optimization work is needed in the future.

Table 1 Dimensions and properties for pontoons and bridge

	Small pontoon	Large pontoon
Length [m]	60	80
Width [m]	22	31
Draft (D) [m]	6	6
Height (H) [m]	9	9
C.O.G of pontoons [m]	-2	-2
GM_{xx} [m]	3	7.4
GM_{yy} [m]	35.5	64.6
Pontoon self-weight [ton]	2319	3933
	Bridge deck	
Bridge weight * [ton/100 m]	3990	
C.O.G of bridge deck [m]	5	
*: bridge weight is estimated based on 100 m length bridge beam		

For single small pontoon, the initial transverse (in y direction) metacentric height is only 3m, which means the transverse stability may not be sufficient if the bridge deck is high, e.g. considering the ship passing by clearance. In this case, three small pontoons together with the upper bridge deck can be constructed and towed as one piece to provide additional transverse stability. Without consideration of upper bridge weight, the C.O.G is assumed to be -2 m from the still water line

(SWL). With the bridge deck C.O.G about 5 m, the total C.O.G can be not so high.

GZ curve represents the righting arm if the pontoon has a heeling angle. The GZ curves for small and large pontoons are shown in Figure 3. The longitudinal (in x direction) GZ curve is much larger than that in the transverse direction (y direction). For small pontoons, the GZ curve is smaller than that for large pontoons. With the increase of C.O.G, the GZ values are reduced.

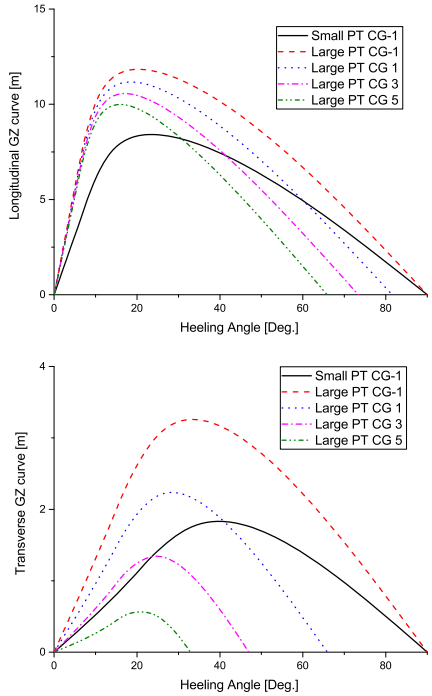

Figure 3 Transverse (top) and longitudinal (bottom) GZ curves for small and large pontoons with changing C.O.G

HYDRO-STRUCTURAL NUMERICAL MODELLING OF THE FLOATING BRIDGE

In this study, numerical modelling considering both hydrodynamic and structural dynamic properties are established. The global dynamic equilibrium of the structural finite element formulation [7] can be expressed as

$$\mathbf{R}^{\mathrm{I}}(\mathbf{r},\ddot{\mathbf{r}},t)+\mathbf{R}^{\mathrm{D}}(\mathbf{r},\dot{\mathbf{r}},t)+\mathbf{R}^{\mathrm{S}}(\mathbf{r},t)=\mathbf{R}^{\mathrm{E}}(\mathbf{r},\dot{\mathbf{r}},t)$$

In which, $\mathbf{R}^{\mathrm{I}}$ is the inertia force vector, including the bridge structural mass, pontoon structural mass and added mass of the pontoons. $\mathbf{R}^{\mathrm{D}}$ is the damping force vector, including the structural internal damping, and wave damping from pontoons due to radiation. $\mathbf{R}^{\mathrm{S}}$ is the stiffness force vector, including the structural internal stiffness and the hydrostatic stiffness. $\mathbf{R}^{\mathrm{E}}$ is the external force vector, considering the gravity and buoyancy force, external specified force or displacement, and the hydrodynamic excitation forces on the pontoons.

Hydrodynamic properties for the pontoons are calculated in frequency domain through Boundary Element Method [8] based on potential flow assumption. In this stage of study, hydrodynamic coupling effect is not considered. Hydrodynamic properties of single pontoon is calculated together with mean drift loads. The hybrid frequency-time domain method [9] is applied to solve the hydrodynamic response of the pontoons based on the Cummin's function [10] taking into consideration of the wave memory effect. Linear hydrodynamic properties are considered with nonlinear viscous effect in the pontoon rigid body motion equations. For a single pontoon, the inertia, viscous, stiffness and memory effect matrix terms are expressed as $\left(\mathbf{M}+\mathbf{A}(\infty)\right)\ddot{\mathbf{r}}_{\mathrm{pt}}(t)$, $\mathbf{B}\dot{\mathbf{r}}_{\mathrm{pt}}(t)\left|\dot{\mathbf{r}}_{\mathrm{pt}}(t)\right|$, $\mathbf{K}\mathbf{r}_{\mathrm{pt}}(t)$ and $\int_0^t \mathbf{k}(t-\tau)\,\dot{\mathbf{r}}_{\mathrm{pt}}(\tau)d\tau$, respectively, in which $\mathbf{M}$ is the pontoon structural mass matrix; $\mathbf{A}(\infty)$ is the added mass matrix at infinite frequency; $\ddot{\mathbf{r}}_{\mathrm{pt}}$, $\dot{\mathbf{r}}_{\mathrm{pt}}$ and $\mathbf{r}_{\mathrm{pt}}$ are the acceleration, velocity and displacement vector of the pontoon in time domain, respectively; $\mathbf{B}$ is the quadratic viscous damping coefficients matrix; $\mathbf{K}$ is the hydrostatic stiffness; $\mathbf{k}(\tau)$ is the retardation function matrix, which is based on the added mass or wave damping matrix. These terms are directly incorporated in the finite element equilibrium equation as nodal properties. The viscous effect are considered as the quadratic viscous damping coefficient matrix, the quadratic coefficients Cd for surge and sway are assumed to be 0.9, while for heave it is assumed to be 1.2 [11].

For global finite element model, Euler beam element with 6 nodal D.O.F (3 translational and 3 rotational) is used to model the bridge deck. The beam cross section properties can be specified in terms of bridge sectional rigidity. The sectional rigidity refers to EA in the axial direction, EI in bending direction and GJ in torsional direction, where E is the Young's modulus, A is the bridge cross sectional area, I is the area moment of inertia, G is the shear modulus, and J is the torsional constant of the cross section. For simplicity, the rigidities are expressed by KA, KB (KBH, KBV) and KT in the axial, bending (in horizontal X or vertical Z directions) and torsional directions, respectively. In general, nonlinearities of the structural model are mainly due to the geometrical rigidity. In this study, fixed boundary conditions in the 6 D.O.F on the two end nodes of the floating bridge are specified, i.e., it is assumed that the bridge onshore connections are rigid.

Environmental conditions such as wave excitation force, current force or even wind force and traffic loads can be applied on the finite element model as a function of time and displacement. The numerical model is established as shown in Figure 2.

STATIC RESPONSES

The bridge sectional rigidity will directly affect the static deformations under the static loads. Under distributed bridge self-weight and buoyancy forces provided by pontoons, there will be static deformation for the whole bridge deck. In the initial stage, the bridge sectional rigidity values are not known, in this case, an estimated number is used. Based on a rough estimation of the truss section of the floating bridge, the axial rigidity KA is in the level of 10^{11} N or higher, the bending and torsional rigidity KB and KT is in the level of 10^{12} Nm^2 and 10^{11} N m^2/rad or higher. Different levels of rigidities are investigated, and the static deformation of the bridge deck is estimated. The horizontal

and vertical static deformation under the total weight of the bridge are shown in the left and middle plots of Figure 4. It is noted that the values in the legend represents values for all the rigidity parameters, i.e., all the rigidity parameters have the same values as a first estimation. Neglecting the wave current interaction effect, the current load component is also considered as static load in this analysis. A current condition of 2 m/s is investigated, and the current induced bridge horizontal static deformation at the pontoon position is presented in the right plot of Figure 4. It is clear from Figure 4 that the structural rigidity with 10^{10} indicates a very soft bridge so that under these static loads, large deformation will occur. The rigidity level of 10^{12} is an acceptable values from static point of view.

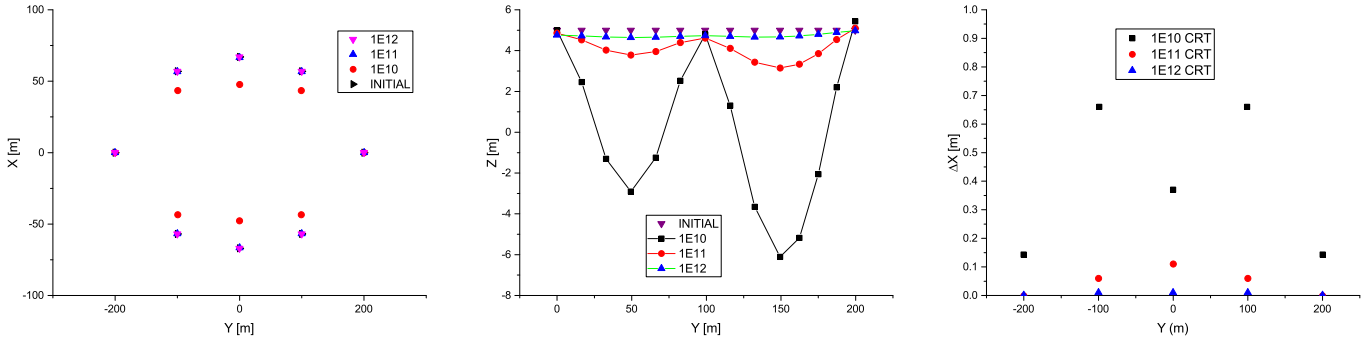

Figure 4 Static deformation in X (left) and Z (middle) directions under self-weight, and static deformation in X direction (right) under static current condition with current velocity of 2 m/s

EIGENVALUE ANALYSIS

For the current concept, eigenvalue analysis is performed based on different bridge sectional rigidity, i.e., KA, KBV, KBH and KT values. Same values apply for all the rigidity parameters, and the first 20 eigenvalue results for different bridge rigidity are shown in Figure 5. It is seen that the first eigenvalues for the structural rigidity with 10^{11}, 10^{12} and 10^{13} are 33s, 9s and 7s respectively. For rigidity level of 10^{12}, the first 3 eigenvalues are around 10s. The first and second eigen-modes for different bridge rigidity levels are shown in Figure 6 and Figure 7, respectively. In these plots, Y represents the Y position of different FEM nodes along the bridge, X represents the displacement in X direction, and Z represents displacement in Z direction under the corresponding eigen-mode. It is noted that in the first eigen-mode, the nodal displacement evolve gradually from X-Y plane to Y-Z plane with the increase of the bridge rigidity. Similar phenomena can be observed in the second eigen-mode. With the bridge rigidity of 10^{13}, the first and second eigen-modes are mainly in Z direction.

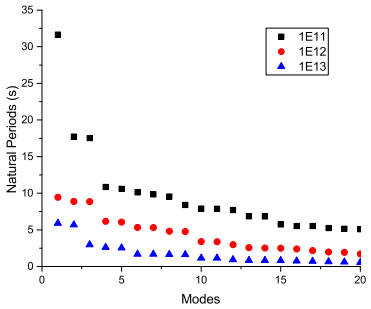

Figure 5 First 20 eigenvalues for different bridge sectional rigidity levels.

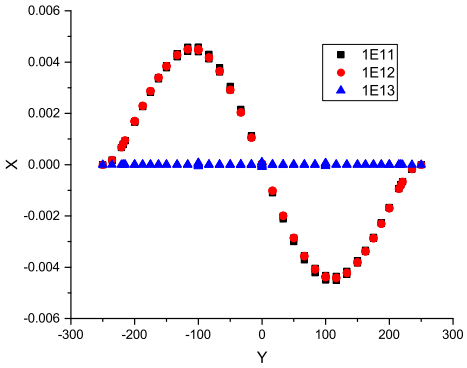

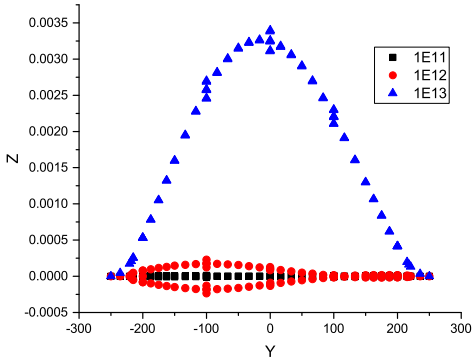

Figure 6 Second eigen-modes in X and Z directions for different bridge sectional rigidity levels

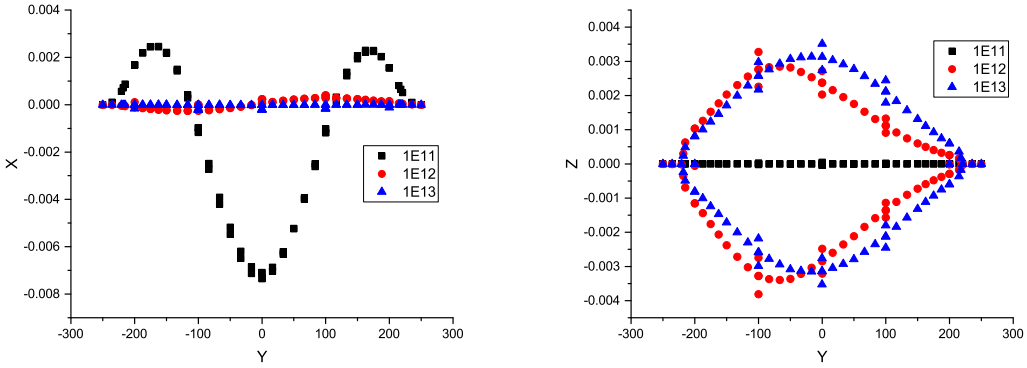

Figure 7 Second eigen-modes in X and Z directions for different bridge sectional rigidity levels.

From design point of view, it is best to avoid the eigenvalues to be located at the wave region with significant energy. In this analysis, no optimization work is done, but these work need to be performed to improve the dynamic properties of the bridge.

HYDRODYNAMIC REPONSES UNDER REGULAR WAVE AND WHITE NOISE WAVE

Bridge rigidity parameters significantly affect the system dynamic response performance. In this case, a sensitivity study is performed in terms of bridge rigidity. Different bridge sectional rigidity parameters are screened in terms of axial KA, vertical bending KBV, horizontal bending KBH and torsional KT. It is assumed in the initial stage design that the cross sectional rigidity parameters are uniform along the whole bridge. In this bridge configuration, the horizontal bending rigidity KBH is assumed to be three times of the vertical bending rigidity KBV. The cross sectional rigidity parameters and the corresponding case number are listed in Table 2. White noise wave is used to study the response of the bridge. The white noise wave covers the range of angular frequency from 0.1 to 5 rad/s, i.e. approximately from 1 s to 60 s, with the same amplitude of 1 m. The response results in surge, heave and pitch for the central pontoon are presented in Figure 8, Figure 9 and Figure 10, respectively together with white noise spectrum. The blue lines represent the wave white noise spectrum which is referred to the right y axis in these plots. It is clear that in all the cases, multiple modes and frequencies are involved in the responses. Different modes are induced based on the combined effects from axial, bending and torsional rigidity, so changing of one parameter is not a feasible way to identify the exact effects. However, the change of different parameters will give an idea how responses are changed.

In Figure 8, when KA is changed from A1 to A3, the surge responses are reduced, and the response frequencies are also altered in a significant way, but the continual change from A3 to A5 does not induce significant change in surge responses. The change of KB and KT also significantly affect the surge responses. In general, with the increase of the rigidity values to a level, the responses are reduced, and continuous increase of the rigidity will not induce significant response difference. The threshold values are the appropriate parameters that can be used in the initial design stage.

Table 2 Structural rigidity parameters studied and the corresponding case numbers

	A1	A2	A3	A4	A5	B1	B2	B3	B4	B5	C1	C2	C3
KA [N]	**1.E+10**	**1.E+11**	**1.E+12**	**1.E+13**	**1.E+14**	1.E+12	1.E+12	1.E+12	1.E+12	1.E+12	1.E+12	1.E+12	1.E+12
KBV [Nm^2]	1.E+12	1.E+12	1.E+12	1.E+12	1.E+12	**1.E+10**	**1.E+11**	**1.E+12**	**1.E+13**	**1.E+14**	1.E+12	1.E+12	1.E+12
KBH [Nm^2]	3.E+12	3.E+12	3.E+12	3.E+12	3.E+12	**3.E+10**	**3.E+11**	**3.E+12**	**3.E+13**	**3.E+14**	3.E+12	3.E+12	3.E+12
KT [Nm^2/rad]	1.E+12	1.E+12	1.E+12	1.E+12	1.E+12	1.E+12	1.E+12	1.E+12	1.E+12	1.E+12	**1.E+11**	**1.E+13**	**1.E+14**

In Figure 9, the change of KA and KT in these levels has no effect on heave motions, while KB has the most significant effect. It means the bending rigidity of the bridge deck rather than the axial and torsional rigidity can induce effective control of the heave motion. In Figure 10, the pitch responses are strongly affected by KB and KT, i.e., bending and torsional rigidity, and are not strongly influenced by the axial ridigity. The increase of the rigidity values induce smaller pitch motions. Based on the previous analysis, the combination values of KA from A3, KB from B4 and KT from C2 could be appropriate initial rigidity values that be applied to the bridge cross section design.

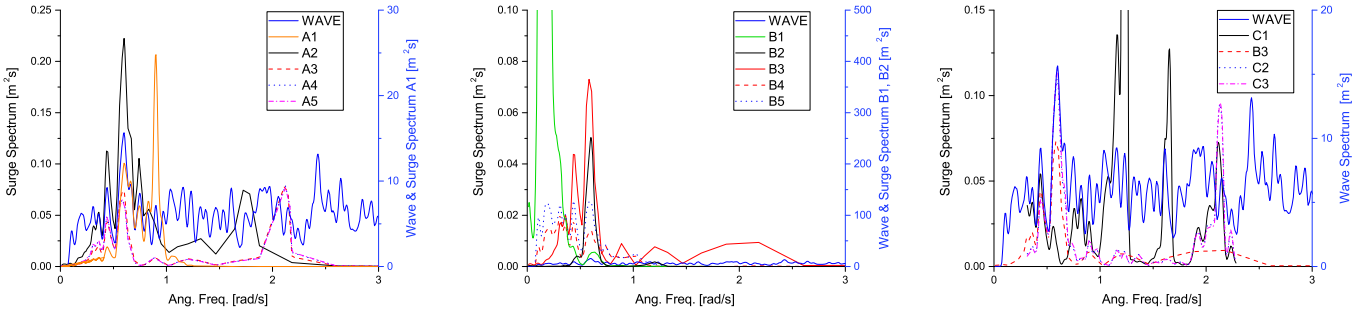

Figure 8 Surge response of the central pontoon 1 for different structural parameter cases under white noise wave excitation

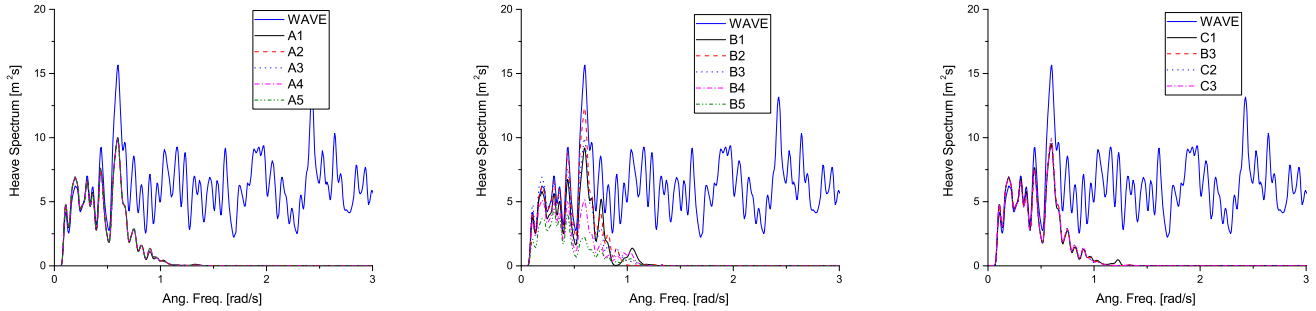

Figure 9 Heave response of the central pontoon 1 for different structural parameter cases under white noise wave excitation

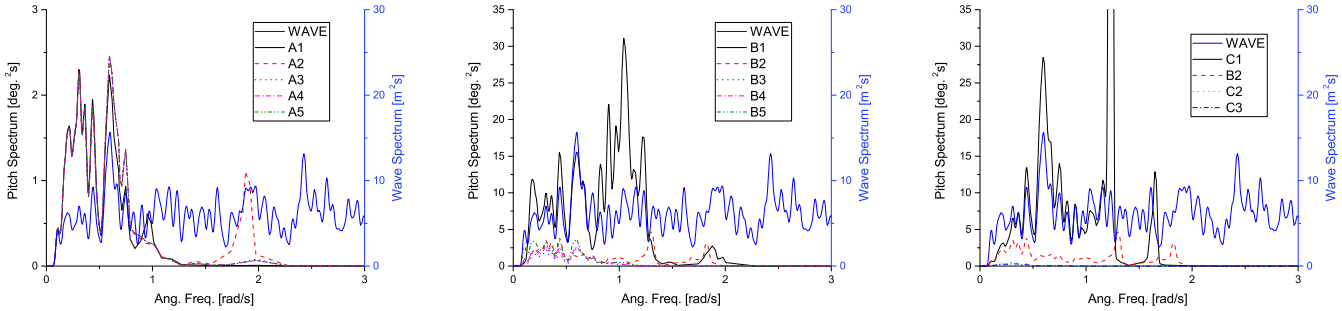

Figure 10 Pitch response of the central pontoon 1 for different structural parameter cases under white noise wave excitation

The responses of the side pontoons are expected to be smaller than that of the central pontoons. The central and side pontoons responses under white noise wave for the case B4 are plotted in Figure 11. For all the D.O.F, the side pontoon responses are always smaller than the central pontoon responses, and the side large pontoons has the smallest responses. It is obvious that the heave motion of the side pontoons are the D.O.F that is most significantly reduced. Different regular wave periods are also investigated for the case with rigidity level of KA 10^{12}, KBH 10^{13} and KT 10^{13}, and the motion RAO of the central, Y positive, and Y positive side pontoons (CTRL PT1, YPOS PT1 and YPOSSIDE PT) are presented in Figure 12. The same conclusions as for the white noise wave case can be drawn. In addition, larger responses for surge and pitch can be observed with the increase of wave periods, and there is a peak in heave motion response at around 13 s.

The end connections are the critical part in this bridge design. The structural element forces for the same case as in Figure 12 are investigated under different regular wave periods. The structural response results including axial force, bending moment, shear force and torsional moment are presented in Figure 13 and Figure 14. It is obvious that the bending moment M_{xx} and shear force Fs_{zz} in the vertical direction is larger than M_{zz} and Fs_{xx} that in the horizontal directions, and the structural responses in the end part are generally larger than the responses in the central part. These results provide indications and input for the structural design.

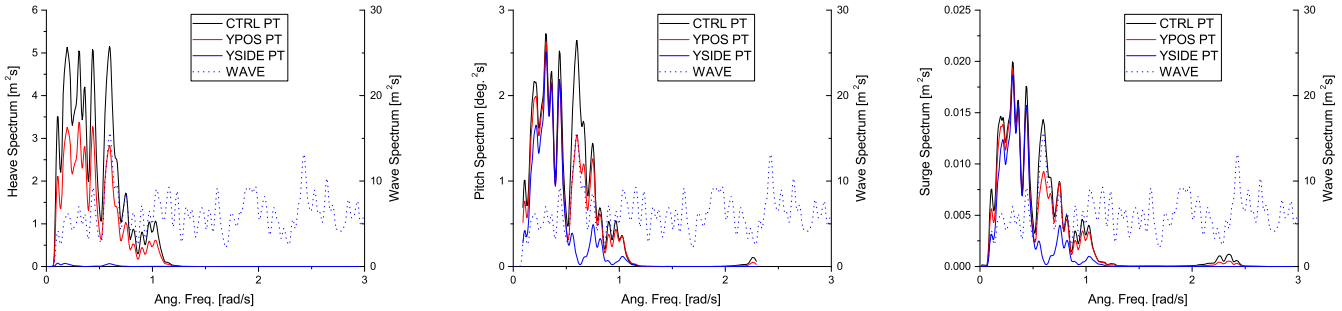

Figure 11 Surge (left), heave (middle) and pitch (right) response of the different pontoons under white noise wave excitation

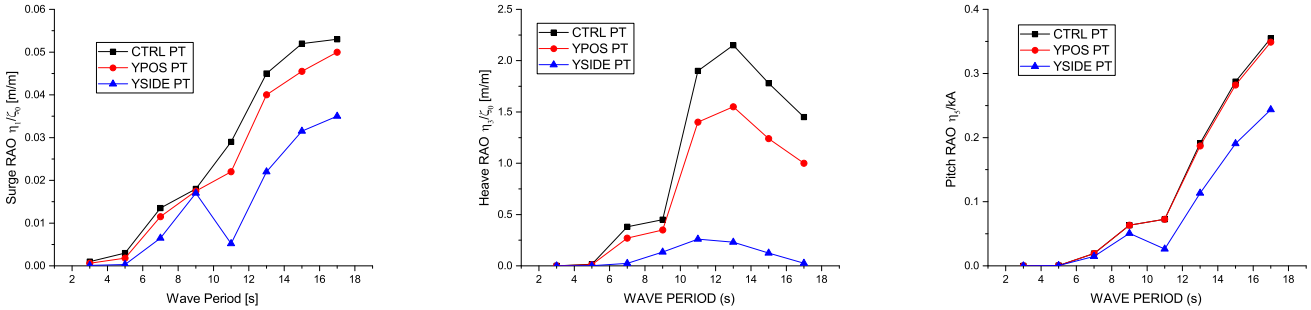

Figure 12 Surge (left), heave (middle) and pitch (right) RAO of the different pontoons under different regular wave cases

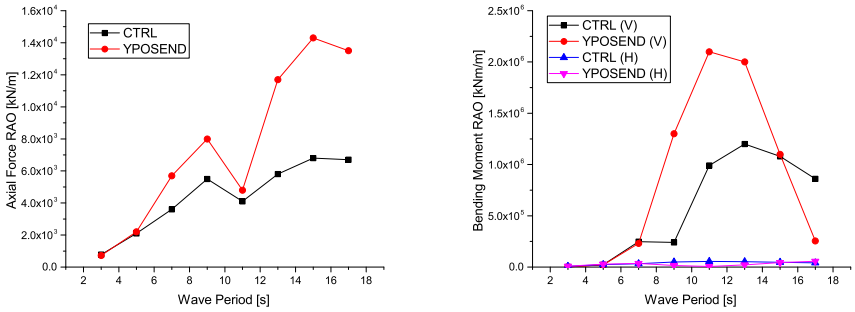

Figure 13 RAOs of the axial force and bending moment in vertical (Z) and horizontal (X) directions

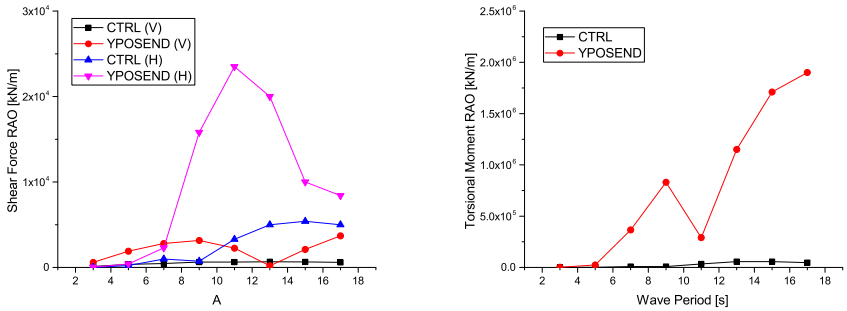

Figure 14 RAOs of the shear force in vertical (Z) and horizontal (X) directions and torsional moment

HYDRODYNAMIC RESPONSES UNDER IRREGULAR WAVE CONDITIONS

The performance of the bridge under different sea states is investigated in this part. In this study, 1 year return period and 100 year return period sea states are specified as Hs=1m, Tp=5s and Hs=2m, Tp=7s, respectively. The wave spectrum is assumed to follow JONSWAP spectrum, with peakedness parameter γ equals 3.3. In this part, one hour simulation results are used for analysis. The rigidity parameters studied in the irregular wave analysis are KA equals 10^{12}, KBH equals 10^{13} and KT equals 10^{13}.

The motion and acceleration statistical results in surge, heave and pitch of all the pontoons under the sea state with Hs=1m and Tp=5s are presented in Figure 15 and Figure 16, respectively. For the serviceability of the floating bridge, dynamic responses should satisfy design criteria to ensure comfort driving [2]. Under 1 year storm (Hs=1m and Tp=5s) wave dynamic actions, the surge, heave and pitch deflections should be in the range of ±0.3 m, ±0.3 m and ±0.5 degrees, respectively, and the corresponding accelerations should be in the range of ±0.5 m/s^2 , ±0.5 m/s^2 and ±2.87 degree/s^2. Based on these criteria, it can be seen from Figure 15 and Figure 16 that the responses satisfy the serviceability requirement.

The motion statistical results of all the pontoons under sea state of Hs=2 m, and Tp=7 s are presented in Figure 17. The spectral results of the three pontoons CTRL1, YPOS1, and YPOSSIDE as well as the wave spectrum are shown in Figure 18. It can be seen that under the sea state with 100 year return period, the heave responses has exceeded the serviceability criteria. The spectral results show that the motion responses are located in wave frequency region, and two response peaks are clearly observed in surge and pitch.

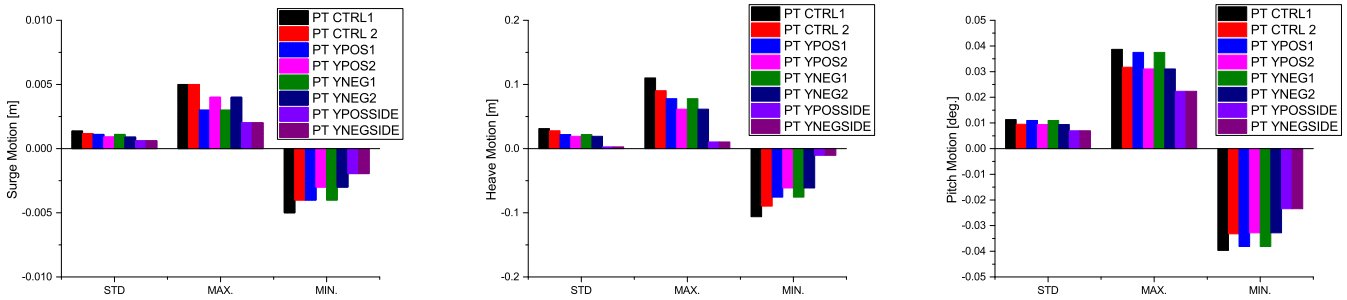

Figure 15 Statistical results (STD, MAX. and MIN.) in surge, heave and pitch motions of all the pontoons under sea state with Hs=1 m and Tp= 5s

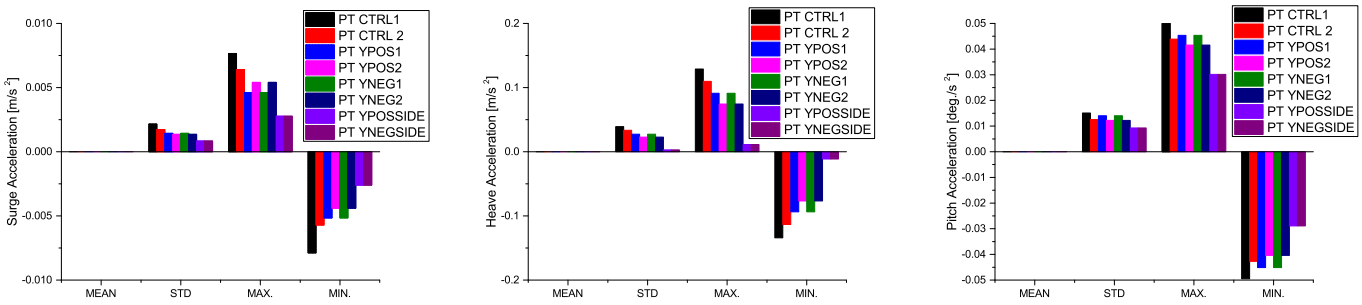

Figure 16 Statistical results (STD, MAX. and MIN.) in surge, heave and pitch accelerations of all the pontoons under sea state with Hs=1 m and Tp= 5s

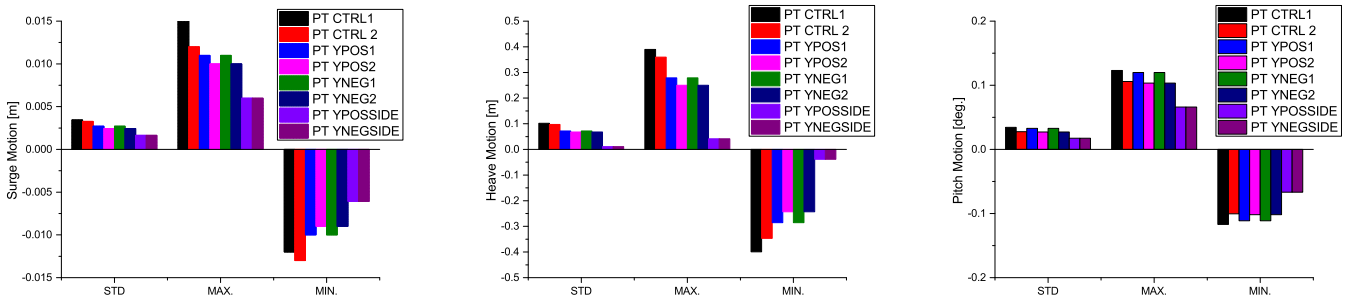

Figure 17 Statistical results (STD, MAX. and MIN.) in surge, heave and pitch motion of all the pontoons under sea state with Hs=2 m and Tp= 7s

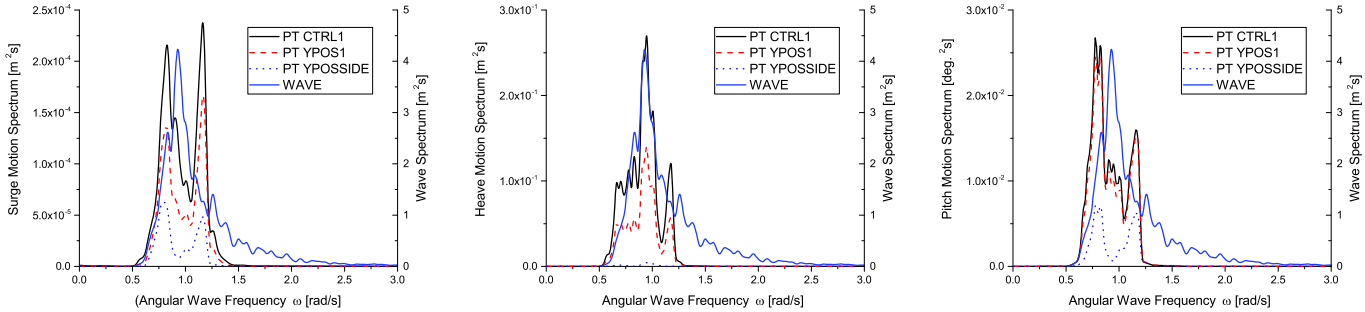

Figure 18 Spectral of surge, heave and pitch motion of the CTRL1, YPOS1 and YPOSSIDE pontoons under sea state with Hs=2 m and Tp= 7s, and wave spectrum.

CONCLUSION AND RECOMMENDATIONS FOR FUTURE WORK

This paper deals with the initial design of a double curved floating bridge, involving stability of the pontoons and defining the C.O.G limit in the construction and installation phase. Parametric study are carried out in terms of the bridge structural rigidity firstly in static analysis, in eigenvalue analysis and then in dynamic global response analysis. Based on the motion analysis under white noise wave, structural rigidity are recommended for the bridge. Further dynamic response analysis are performed under regular wave and irregular wave conditions. Statistical and spectral results are presented.

It is found from the static analysis that the bridge deck rigidity level of 10^{12} is an acceptable values to ensure there is no excessive static bridge deformation. Current induced static deformation under this rigidity level is so small that it can be neglected. In the eigen value analysis, it is found that the bridge structural rigidity can have strong effect on the eigen values. With the structural rigidity change from 10^{11} to 10^{13} levels, the first two eigen-modes tend to transfer from X-Y plane to Y-Z plane. Further optimization work need to be carried out to avoid the eigen-modes to be located in the wave region with significant energy. From dynamic analysis, different structural rigidity values are screened based on the white noise wave, and found that pontoon motions are strongly affected by the structural rigidity. In general, the higher the rigidity, the smaller the motions. But threshold values for the rigidity exist that when the values are exceeded, the motion is not strongly affected. In the rigidity levels investigated, the surge motions are strongly affected by all the axial, bending and torsional rigidity. The heave motions are significantly affected by the bending rigidity. The pitch motions are strongly affected by the bending and torsional rigidity. Based on the parametric study, appropriate rigidity levels are selected.

Among all the pontoons, the motions of side pontoons are smaller than the central pontoons, the large side pontoons have the smallest motions. Heave motions are the D.O.F that are most significantly affected. Based on the regular wave analysis, it is found that the bending moment and shear force in the vertical direction is larger than that in the horizontal directions, and the structural responses in the end part are generally larger than the responses in the central part.

Based on the selected structural rigidity in the axial, horizontal bending, torsional directions, i.e., KA equals 10^{12}, KBH equals 10^{13} and KT equals 10^{13}. Irregular wave conditions with 1 year return period and 100 years return period are studied, and statistical and spectral analysis are performed. Under 1 year return period sea state, the motion responses satisfy the serviceability criteria, ensuring the driving comfort. While under 100 year return period sea state, the heave motion exceeds the driving comfort criteria.

In the near future, optimization work in terms of pontoon size, pontoon spacing, as well as bridge structural rigidity need

to be done to ensure good dynamic bridge properties. Dynamic traffic load should also be considered in the dynamic response analysis. In addition, hydrodynamic coupling effect should be incorporated in the analysis. Model test of the floating bridge can be performed to validate the numerical model.

ACKNOWLEDGEMENT

The author gratefully acknowledge the financial supports from the Multi-Purpose Floating Structure (MPFS) project, from the JTC through the Center for Offshore Research & Engineering (CORE), National University of Singapore. Dr Jiang Dongqi, and Dr Hu Cun are also acknowledged for their inspiring discussion during this study.

REFERENCES

[1] Lwin, M., Floating bridges. Bridge Engineering Handbook, 2000. 22: p. 1-23.
[2] Watanabe, E. and T. Utsunomiya, "Analysis and design of floating bridges". Progress in Structural Engineering and Materials, 2003. 5(3): p. 127-144.
[3] Solland, G., S. Haugland, and J.H. Gustavsen, "The Bergsøysund Floating Bridge", Norway. Structural Engineering International, 1993. 3(3): p. 142-144.
[4] Norwegian Public Roads Administration, A feasability study - How to cross the wide and deep Sognefjord. 2011.
[5] Watanabe, E., T. Utsunomiya, and C. Wang, "Hydroelastic analysis of pontoon-type VLFS: a literature survey". Engineering structures, 2004. 26(2): p. 245-256.
[6] Fredriksen, A.G., et al., "Comparison of global response of a 3-span floating suspension bridge with different floater concepts". Proceedings of the 35th International Conference on Ocean, Offshore and Arctic Engineering, 2016.
[7] MARINTEK, RIFLEX Theory Manual V4.0 rev3. 2013.
[8] Faltinsen, O.M., Sea loads on ships and offshore structures. Vol. 1. 1993: Cambridge university press.
[9] Naess, A. and T. Moan, Stochastic dynamics of marine structures. Cambridge University Press. 2013.
[10] Cummins, W., "The impulse response function and ship motions". SchiffStechnik,, 1962. 47(9): p. 101-109.
[11] DNV, Recommended practice dnv-rp-c205, environmental conditions and environmental loads. 2010.